

Carrier Wave Shocking of Femtosecond Optical Pulses

R. G. Flesch, A. Pushkarev, and J. V. Moloney

Arizona Center for Mathematical Sciences, Department of Mathematics, University of Arizona, Tucson, Arizona 85721
(Received 20 June 1995)

Numerical integration of Maxwell's equations for propagation of a femtosecond pulse in a medium with linear Lorentz response and a Kerr nonlinearity shows shock formation on the underlying carrier wave prior to the envelope shock. The carrier shock is characterized by the appearance of a strong third harmonic pulse, whereas the envelope shock appears later as spectral broadening and modulation of the fundamental and higher harmonic spectral features.

PACS numbers: 42.65.Ky

Advances in laser technology in the past decade have made possible the production of pulses which contain a few optical cycles [1]. Although such ultrashort pulses contain small amounts of optical energy, enormous intensities exceeding 1 TW/cm^2 can arise and the accompanying intensity-dependent corrections to the index of refraction are such that one can expect novel nonlinear phenomena such as shock formation over very short propagation lengths. It has been suggested in [2] that an envelope shock was observed experimentally [3] and that this can be understood using standard envelope approximations [2,4] to Maxwell's equations. Laser-induced breakdown (LIB) cannot be ruled out at such very high peak intensities, but there is evidence to show that for such short and hence low energy pulses the cascade-avalanche path is unlikely and multiphoton processes are more likely to lead to breakdown [5]. Indeed, very recent experiments in water using 100 fs pulses indicate that local peak field intensities can exceed 10^{13} W/cm^2 in the focal region with incident pulse absorption being less than 5% [6]. Moreover, breakdown becomes a sensitive function of optical wavelength. Shock formation on the carrier wave is expected therefore to compete with other physics during the critical collapse of femtosecond duration optical pulses in optically transparent media where the local intensity at the critical collapse distance can become very large.

The above breakdown scenario is extremely complicated, so we confine our attention here to plane wave propagation for simplicity and show that an optical carrier shock can arise in a medium with an instantaneous Kerr nonlinearity. Dispersion plays an important role in shock regularization (smoothing) and influences the signature of the carrier shock. As dispersion is typically strong for such short optical pulses [the dispersion length scales as k''/τ_p^2 , where k'' is the leading order contribution to the group velocity dispersion (GVD) and τ_p is the characteristic pulse length], phase mismatch leads to the separation in time of a strong third harmonic optical pulse moving with a different group velocity from the fundamental. For very weak dispersion, a component of the third harmonic pulse moves with the fundamental and, in the dispersionless case, all higher harmonics of the fundamental are phase matched

and see explosive growth. As the phenomena we are concerned with occurs on the scale of the carrier wavelength, no envelope approximations are valid and one must resort to a numerical integration of Maxwell's equations. Numerical schemes for the integration of Maxwell's equations have been refined in the past few years [7] to allow for an efficient integration of media with memory in both the linear and nonlinear polarizations.

We restrict our attention to nonmagnetic dielectric media with no free charges, in which case we have for Maxwell's equations

$$\frac{\partial B_y}{\partial t} = \frac{\partial E_x}{\partial z}, \quad \frac{\partial D_x}{\partial t} = \frac{1}{\mu_0} \frac{\partial B_y}{\partial z}, \quad (1)$$

where all quantities above and in the following are in MKS units. The medium is modeled by a single Lorentz oscillator plus an instantaneous Kerr nonlinearity

$$D_x(z, t) = \epsilon_0 \left\{ \epsilon_\infty E_x(z, t) + \int_{-\infty}^t dt' \chi(t-t') E_x(z, t') + \chi^{(3)} E_x^3(z, t) \right\}, \quad (2)$$

with the linear susceptibility given by $\chi(t) = \omega_p^2 e^{-\delta t/2} \times \sin(\sqrt{\omega_0^2 - \delta^2/4} t) / \sqrt{\omega_0^2 - \delta^2/4}$, $[\hat{\chi}(\omega) = \omega_p^2 / (\omega_0^2 - i\delta\omega - \omega^2)]$, $\omega_p^2 = (\epsilon_s - \epsilon_\infty)\omega_0^2$, ϵ_s and ϵ_∞ are the static and infinite relative permittivities, respectively, and ω_0 the resonance frequency of the Lorentz oscillators. Maxwell's equations are solved by either a second order in time, second order in space [(2,2)] finite difference time domain method [8] or a second order in time, fourth order in space [(2,4)] scheme [9]. The numerical dispersion inherent in these methods has recently received a good deal of attention [10], and we have chosen our spatial discretizations accordingly.

The convolution integral $P_L = \epsilon_0 \int dt' \chi(t-t') E_x(t')$ in Eq. (2) is most efficiently solved by replacing it with the equivalent second order ordinary differential equation [7,11]

$$\frac{1}{\omega_0^2} \frac{d^2 P_L}{dt^2} + \frac{\delta}{\omega_0^2} \frac{d P_L}{dt} + P_L = \frac{\omega_p^2}{\omega_0^2} \epsilon_0 E_x, \quad (3)$$

which is solved by second order central differencing.

Ignoring dispersion initially we obtain a prediction for the carrier shock formation time. For this case and for later analysis it is useful to recast the coupled equations as a second order integro-differential equation

$$\frac{\partial^2 E_x}{\partial t^2} - \epsilon_\infty c^2 \frac{\partial^2 E_x}{\partial z^2} - \chi^{(3)} \frac{\partial^2 E_x^3}{\partial t^2} - \frac{\partial^2 P_L}{\partial t^2} = 0, \quad (4)$$

where c is the speed of light in vacuum. Closely connected with Eq. (4) in the case of zero dispersion ($P_L = 0$, $\epsilon_\infty = 1$) is the following transport equation:

$$\frac{\partial E_x}{\partial t} - C(E_x) \frac{\partial E_x}{\partial z} = 0, \quad (5)$$

with the amplitude-dependent velocity $C(E_x)$ given by $C(E_x) = c/\sqrt{1 + 3\chi^{(3)}E_x^2}$. Using this relation and its first time derivative to eliminate all time derivatives in Eq. (4) (with $P_L = 0$) one can show that any solution of Eq. (5) is a solution of the Maxwell Eq. (4). Equation (5) has shock solutions [12], and the time for the wave to break is given by

$$t_B = -\left(\frac{d}{d\xi} F(\xi) \Big|_{\xi=\xi_B}\right)^{-1}, \quad (6)$$

where $F(\xi) \equiv C[E_x(\xi, 0)]$ and ξ_B denotes the value of ξ for which $F'(\xi) < 0$ and $|F'(\xi)|$ is a maximum.

Carrier shock breaking times were confirmed by solving the system Eqs. (1) and (3) numerically. As an initial condition we choose a 30 fs Gaussian pulse (FWHM) of amplitude E_0 and carrier frequency $\omega_c = 4.0 \times 10^{14}$ ($T_{\text{opt}} = 15.7$ fs). The Kerr medium used has a dimensionless strength $\chi^{(3)}E_0^2 = 0.022$. In Fig. 1 we show the pulse profile shortly after having entered the Kerr medium

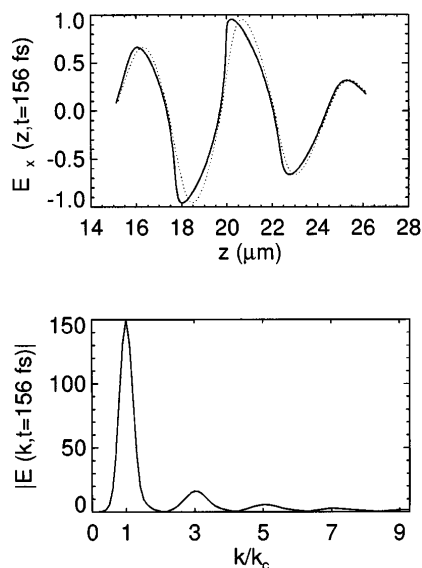


FIG. 1. A 30 fs pulse after propagating 6.8 (dotted) and 20.2 μm (solid) in a dispersionless medium with Kerr nonlinearity 0.022. The dotted curve has been translated so as to coincide with the breaking wave form.

and a second profile (solid) after the pulse has propagated 20 μm . Carrier shock formation is clearly evident, the strongest shock occurring where the pulse has maximum amplitude. The spatial Fourier transform shows the presence of multiple harmonics due to exact phase matching for this dispersionless medium.

Figure 2 shows numerically determined breaking times for different values of the dimensionless Kerr strength $\chi^{(3)}E_0^2$. The pulse initial conditions were the same as above. The solid line is the curve determined by inserting our initial condition into Eq. (6) which yields

$$T_B^c = \frac{1}{3\pi} \frac{T_{\text{opt}}}{\chi^{(3)}E_0^2} \frac{(1 + 4.5\chi^{(3)}E_0^2)^{3/2}}{\sqrt{(1 + 3\chi^{(3)}E_0^2)(1 + 6\chi^{(3)}E_0^2)}} \xrightarrow{\chi^{(3)}E_0^2 \rightarrow 0} \frac{1}{3\pi} \frac{T_{\text{opt}}}{\chi^{(3)}E_0^2}. \quad (7)$$

In arriving at Eq. (7) we have assumed that the pulse width T_{FWHM} is longer than the optical period T_{opt} . The agreement between the numerical values and Eq. (7) is quite good for all but the largest values of $\chi^{(3)}E_0^2$. The deviation for larger values can in part be attributed to the fact that the predicted values assume that the pulse is always in the Kerr medium, whereas in the numerical simulations the pulse enters from vacuum. For larger Kerr strengths the breaking occurs so rapidly that this difference is important.

To contrast carrier shock formation with the more well known envelope shock [1,2], we solved the envelope equation, obtained by inserting the standard ansatz

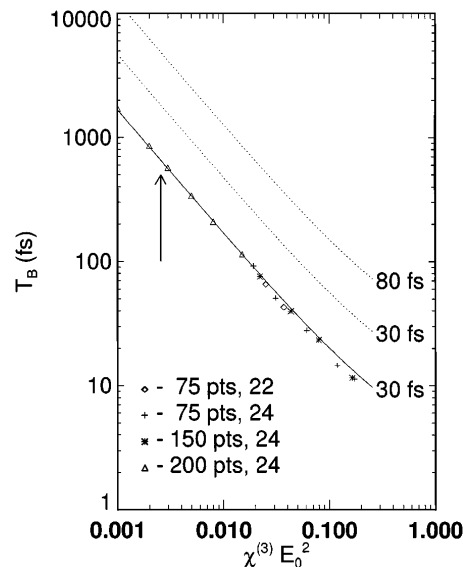


FIG. 2. Numerically determined breaking times as a function of the nonlinearity. Different symbols denote different spatial resolutions and use of either the (2,2) or (2,4) numerical scheme. The formula in Eq. (7) is represented by the solid and dotted lines, respectively, for the pulse widths indicated.

$E_x(z, t) = E_0(Ae^{i(k_c z - \omega_c t)} + \text{c.c.})$, into Eq. (4) to obtain

$$\begin{aligned} \frac{\partial A}{\partial z} = & -k'_c \frac{\partial A}{\partial t} - \frac{ik''_c}{2} \frac{\partial^2 A}{\partial t^2} + \frac{k'''_c}{6} \frac{\partial^3 A}{\partial t^3} \\ & + \chi^{(3)} E_0^2 \frac{3i\omega_c^2}{2k_c c^2} |A|^2 A - \chi^{(3)} E_0^2 \frac{\omega_c}{2k_c c^2} \\ & \times \left(2 - \omega_0 \frac{k'_c}{k_c} \right) \frac{\partial |A|^2 A}{\partial t}, \end{aligned} \quad (8)$$

where $k_c^2 c^2 = \omega_c^2 n(\omega_c) = \omega_c^2 [1 + \hat{\chi}(\omega_c)]$ and primes denote derivatives with respect to ω . The last term in Eq. (8) gives rise to the envelope shock. One can explicitly derive an envelope breaking time if the GVD term (k''_c) is small relative to the shock term. Following the same analysis which leads to Eq. (7) we obtain $T_B^e = 0.156cT_{\text{FWHM}}/\chi^{(3)}E_0^2 v_p(2 - v_p/v_g)$, where v_p and v_g are the phase and group velocities at the carrier frequency. In physically relevant situations $\chi^{(3)}E_0^2 \ll 0.1$ and we obtain the simple ratio for the carrier and envelope breaking times $T_B^e/T_B^c \approx 1.467T_{\text{FWHM}}/T_{\text{opt}}$ where we have taken $v_p = v_g = c$ due to the small dispersion. Since the envelope approximation is only valid when the pulse contains at least two optical cycles, we see that the time

for the envelope to break is always much longer than the breaking time for the carrier.

To avoid long computations and accumulation of numerical dispersion errors we have used a Kerr strength of $\chi^{(3)}E_0^2 = 0.01$ ($\delta n = 3\chi^{(3)}E_0^2/8n_0 = 0.0034$), but as the plot in Fig. 2 indicates, the carrier shocking phenomena scales to nonlinear index changes on the order of 10^{-4} . Figure 3 shows a direct comparison of the evolution of an 80 fs pulse for the 1D vector Maxwell and the envelope model [Eq. (8)] in a Lorentz medium with a GVD of $2.5 \text{ ps}^2/\text{km}$ [13]. The envelope solution appears as a smooth curve superimposed on the oscillatory optical carrier pulse solution to Maxwell's equations. The accompanying pulse power spectra show the appearance of a strong third harmonic component characteristic of the carrier shock. Higher harmonics are suppressed by the small GVD present which prevents the carrier wave from breaking as is shown in Fig. 1. In Fig. 4 the pulse has propagated $525 \mu\text{m}$, and we see the development of an envelope shock accompanied by the strong spectral broadening and modulation. On the trailing edge one can see that the third harmonic pulse generated by the carrier shock is beginning to separate from the fundamental due to the difference in

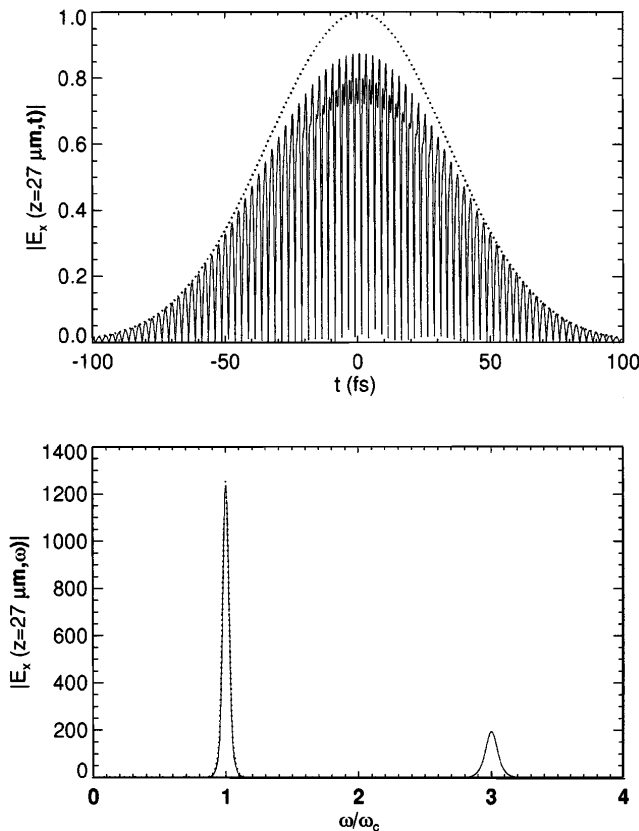


FIG. 3. Comparison of the envelope approximation with the 1D Maxwell's equation after propagating $27 \mu\text{m}$. The appearance of the strong third harmonic in the Maxwell spectrum indicates the presence of a carrier shock. Note that the Fourier transform for the envelope has been shifted by ω_c to facilitate comparison.

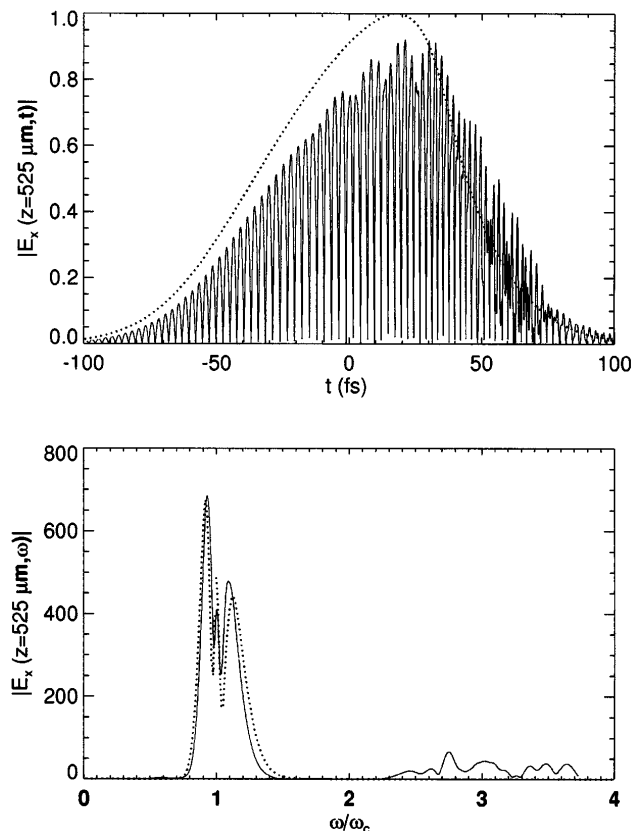


FIG. 4. As in Fig. 3 after propagating $525 \mu\text{m}$. An envelope shock has developed on the trailing edge of the pulse which is reflected in the strong spectral broadening in the Fourier spectrum. The third harmonic pulse separates from the fundamental, and both fundamental and third harmonic spectra are strongly modulated.

group velocities at the fundamental and third harmonic. Since the GVD used is quite small, the estimated distances for carrier and envelope shocks (117 and 377 μm , respectively) are still useful as they indicate the approximate distances at which the shocks appear. We remark that at a GVD of 52 ps^2/km the same features are evident, but now the third harmonic pulse generated by the carrier shock is smaller than the fundamental by a factor of 25 (in Fig. 3, the difference is a factor of 6).

We have shown that novel nonlinear self-steepening effects can act in concert to produce two well separated self-steepening events, one on the optical carrier and the other on the envelope of the carrier (when this is well defined) as an intense many-femtosecond duration optical pulse propagates in optically transparent media. Carrier shocking and dispersive regularization are bound to play a key role, competing with many other complex physical processes, during femtosecond pulse critical collapse in bulk transparent media. Unlike the case considered here, the shock time, or equivalently shock distance, will become an extremely sensitive function, decreasing rapidly as the critical collapse point is approached. In 1D, the experimental results of Knox *et al.* [3] show a maximum nonlinear index change of 6.4×10^{-3} which is within the range of nonlinearities we have studied (see arrow in Fig. 2). A value of n_2 2 orders of magnitude larger than that of silica has recently been reported [14] and is a good candidate material for demonstration of carrier shocks. With the currently available short pulsed lasers one should be able to see the harmonic signature of the carrier shock even for silica. The standard Sellmeier formula for silica [2,15] yields a ratio of the phase to group velocity near unity near $\lambda = 620 \text{ nm}$ which is the carrier wavelength used by Knox *et al.* It is therefore possible that any higher harmonics that they may have observed are, in fact, the carrier shock signature. The fringe-resolved autocorrelation (FRAC) technique [16] may provide direct measurements of the carrier shock formation. A more realistic model for silica would require our replacing the single resonance Lorentz model with a corresponding three resonance Sellmeier model. This would allow much

more flexibility in varying the GVD and the phase-group velocity mismatch.

The authors acknowledge support from the Arizona Center for Mathematical Sciences under Contracts No. AFOSR F49620-94-1-0051 and No. AFOSR F49620-94-1-0463.

-
- [1] *The Supercontinuum Laser Source*, edited by R. R. Alfano (Springer-Verlag, New York, 1989).
 - [2] G. P. Agrawal, *Nonlinear Fiber Optics* (Academic Press Inc., Boston, 1989), Chap. 4.
 - [3] W. H. Knox, R. L. Fork, M. C. Downer, R. H. Stolen, and C. V. Shank, *Appl. Phys. Lett.* **46**, 1120 (1985).
 - [4] F. Demartini, C. H. Townes, T. K. Gustafson, and P. L. Kelley, *Phys. Rev.* **164**, 312 (1967).
 - [5] L. V. Keldysh, *Sov. Phys. JETP* **20**, 1307 (1965).
 - [6] P. K. Kennedy, *IEEE J. Quantum Electron.* (to be published).
 - [7] R. M. Joseph, S. C. Hagness, and A. Taflove, *Opt. Lett.* **18**, 1412 (1991); P. M. Goorjian, A. Taflove, R. M. Joseph, and S. C. Hagness, *IEEE J. Quantum Electron.* **28**, 2416 (1992); P. M. Goorjian and A. Taflove, *Opt. Lett.* **17**, 180 (1992); R. M. Joseph, P. M. Goorjian, and A. Taflove, *Opt. Lett.* **18**, 491 (1993).
 - [8] Kane S. Yee, *IEEE Trans. Antennas Propag.* **AP-14**, 302 (1966).
 - [9] J. Fang, Ph.D. dissertation, Department of Electrical Engineering, University of California, Berkeley, CA, 1989.
 - [10] K. L. Shlager *et al.*, *IEEE Trans. Antennas Propag.* **41**, 1732–1737 (1993); P. G. Petropoulos, *IEEE Trans. Antennas Propag.* **42**, 859–862 (1994); **42**, 62–69 (1994).
 - [11] J. D. Jackson, *Classical Electrodynamics* (Wiley, New York, 1975), 2nd ed.
 - [12] G. B. Whitham, *Linear and Nonlinear Waves* (Wiley, New York, 1974).
 - [13] L. G. Cohen, W. L. Mammel, and S. J. Jang, *Electron. Lett.* **18**, 1023 (1982).
 - [14] M. Asobe, K. Suzuki, T. Kanamori, and K. Kubodera, *Appl. Phys. Lett.* **60**, 1153 (1992).
 - [15] D. Marcuse, *Light Transmission Optics* (Van Nostrand Reinhold, New York, 1982), Chaps. 8 and 12.
 - [16] A. Stingl, M. Lenzner, Ch. Spielmann, and F. Krausz, *Opt. Lett.* **20**, 602 (1995).